Smart and Quantitative Near-Infrared Point-Diffraction Interferometer Based on the Self-Referencing Wavefront Sensor

Yang Pengqian[1,2]   Stefan Hippler[3]   Casey Deen[3]   Wolfgang Brandner[3]

Sarah Kendrew[3]   Miao Jie[1]   Zhang Yanli[1]   Zhu Jianqiang[1]

[1] *Joint Laboratory for High Power Laser Physics，Shanghai Institute of Optics and Fine Mechanics，*
Chinese Academy of Sciences，Shanghai 201800，China

[2] *University of Chinese Academy of Sciences，Beijing 100049，China*

[3] *Max-Planck-Institute for Astronomy，Königstuhl 17，D-69117 Heidelberg，Germany*

Abstract   This paper describes the development of a novel infrared point-diffraction interferometer（IPDI），which can be readily applied to real-time quantitative phase measurement. We generate reference wave with the help of Michelson-like unit combined with a low-pass spatial filter，and extract the phase information using windowed Fourier transform algorithm from single off-axis fringes. The arrangement of the proposed setup offers a quasi-common-path geometry，which could significantly minimize the systematic errors. The proposed method of IPDI is effective and sufficient for the dynamic process measurement of small deformation with higher spatial resolution compared with the conventional off-axis scheme. The feasibility of the proposed setup is demonstrated，followed by methods of reconstruction and system calibration. The nanoscale repeatability is achieved in our experiment.

Key words   measurement；point-diffraction interferometer；beam splitter；off-axis；windowed Fourier transform

OCIS codes   120.3180；120.2650

基于自参考的高精度红外点衍射干涉仪研制

杨朋千[1,2]   Stefan Hippler[3]   Casey Deen[3]   Wolfgang Brandner[3]   Sarah Kendrew[3]

缪 洁[1]   张艳丽[1]   朱健强[1]

[1] 中国科学院上海光学精密机械研究所高功率激光物理联合实验室，上海 201800

[2] 中国科学院大学，北京 100049

[3] 德国马普天文所，Königstuhl 17，D-69117 Heidelberg，德国

摘要   介绍了一种结构简单紧凑、可用于高精度实时相位波前测量的红外点衍射干涉仪，采用类迈克耳孙的光学结构，并结合低通小孔滤波，同时使用窗口傅里叶变换的方法解调单幅离轴载波条纹。与传统波前测量技术相比，所提出的准共光路的光学系统结构有效地抑制了系统像差及外部环境干扰等对测量结果的影响，实现高精度和高分辨率的波前探测。实验结果表明，该方法能够实现高精度的相位测量，且其重复精度达到了纳米量级。

关键词   测量；点衍射干涉仪；分束器；离轴；窗口傅里叶变换

中图分类号   120.3180；120.2650   **文献标识码**   A   **doi**：10.3788/CJL201340.0508001

1 Introduction

The point diffraction interferometer（PDI）[1~3] is desirable for high-end applications of optical surface quality test and highly accurate measurement of wavefront aberration. The basic principle of point-diffraction interferometer is to generate diffracted wavefront internally，so called self-referencing. Furthermore，most of these setups are built with the

common path interferometric geometry, and both object wave and reference wave travel the same path as opposed to two widely separated paths, such as in the configurations of Twyman-Green, or Mach-Zehnder interferometer. Because of its common path geometry, the PDI is much less sensitive to certain types of environmental disturbances such as mechanical vibration, temperature fluctuations, and air turbulence. These unique features are due to the common path geometry and the reliable phase retrieval algorithm.

The concept of PDI was first described by Linnik, and fully developed by Smartt et al. [1], which was used to test wavefront quality of the astronomical telescopes. Following these pioneering efforts, many attempts have been made to construct the point-diffraction interferometer, particularly designs with wavelength near extreme ultraviolet for the purpose of optical lithography[4,5]. These methods include applying liquid-crystal spatial light modulator[4]; introducing new elements such as Savart plate, holographic, and diffractive optical components to generate phase-shifted interferograms[7~12]; exploring new design principles such as using micro-polarized mask array to replace a mechanical phase-shifting unit in a conventional interferometer design[10]; and employing multiple detectors to record the phase shifting interferograms simultaneously[11]. Besides, Guo et al.[12] applied point diffraction interferometer to microscopy and performed the quantitative phase measurements by adopting the polarization phase-shifting mechanism. Although these systems can either provide a common-path configuration or be used in the off-axis geometry, all of the above methods have been limited to that they either require mechanical phase-shifting unit, holographic elements, or polarized optics. In addition, those methods cannot be used for the broad-spectrum approach due to the dispersion effect of the elements.

Recently, windowed Fourier phase interferometer (WFPI) has been developed in our laboratory for checking the quantitative transmitted wavefront quality of the silicon entrance windows, which will be installed in the next-generation wavefront sensor cryostat for very large telescope instrument (VLTI)[13]. WFPI is a new technique that extends the concept of complex fringe analysis to the spatial domain and measures

quantitative phase distributions from only one spatial interferogram.

In this paper, an infrared point-diffraction interferometer (IPDI) is extended to perform off-axis high resolution phase measurements by adopting localized spatial Fourier transform algorithm. The method combines the principle of the common-path interferometer and the spatial analysis algorithm to realize the dynamic measurement of the phase map. The principle and system layout of the proposed method are presented. The principle of the windowed Fourier filtering algorithm for phase reconstruction is described in detail. To verify the feasibility of the proposed method, we performed an experiment and made stability tests.

2 Optical setup of the IPDI

The optical configuration of the proposed infrared point-diffraction interferometer is sketched in Fig. 1. Briefly, the fiber-coupled near infrared frequency-stabilized laser with a wavelength of 1523 nm is collimated and used to illuminate the sample in transmission. The neutral density filters are used to control the intensity of the laser beam. After the collimated beam passes through the test specimen, a lens (L2) is located behind the test specimen to convert the beam into a converging beam. The converging beam falls onto the infrared non-polarizing cube beam splitter
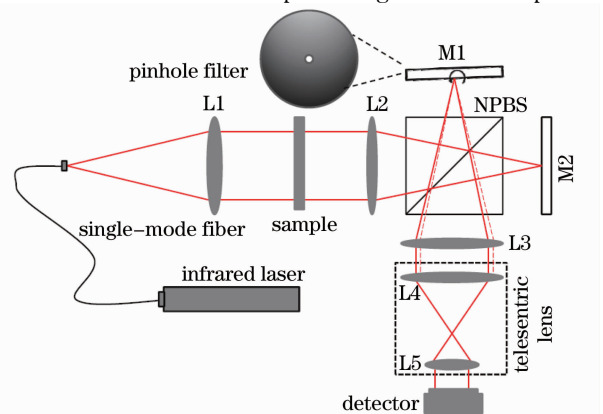

Fig. 1 Experimental setup for slightly off-axis point-diffraction interferometer for compact wavefront measurement with common-path configuration at 1523 nm. L1~L5, achromatic lenses; focal lengths of the lenses $f_1 = 200$ mm, $f_2 = f_3 = 100$ mm, $f_4 = 150$ mm, $f_5 = 45$ mm; the pinhole filter has a diameter of 25 μm.

(NPBS) and then is split into a transmission beam and a reflection beam. The two beams from the beam splitter enter the gold-coated mirrors and are reflected at their Fourier plane，and combined by the beam splitter again. The reflection beam is low-pass filtered by using the pinhole spatial filter positioned in the spatial filter plane，which is the Fourier plane of L2，and transformed as the reference wave. The accuracy of PDI method largely depends on the accuracy of the diffracted spherical wave[10]. To guarantee the quality of the illumination，the pinhole diameter is 25 μm，which is approximately 1. 4 times the half of the Airy disc given by $d = 1.22\lambda f_2/D$，where $\lambda = 1523$ nm is the wavelength and D (10 mm) is the input diameter of the collimated beam. Another lens (L3) is placed in the conjugate position of the first lens (L2) to form a 1:1 $4f$ spatial filtering system. The first lens performs the Fourier transform of the input field of the object，the transformed field is then filtered by the pinhole，and then the product is Fourier transformed again by L3. The normal of the mirror M1 has a small angle with respect to the optical axial direction，thus the reflection beam travels in direction with a small angular offset to the optical axis，and the slightly off-axis fringe pattern is formed. A diaphragm in the Fourier plane of the telescope system is used as the field stop to eliminate ghost images and other unexpected stray light. An infrared camera is located at the back of a $4f$ imaging system to capture the fringe pattern. Since the sample beam only splits at the end of the optical chain，the proposed setup can be considered as a quasi-common-path interferometer，and its stability will be significantly higher compared with conventional interferometers.

3 Wavefront reconstruction

For simplicity，we denoted the object wave after passing through the test specimen as $O_o(x,y)$. Considering a tilted angle introduced by mirror M1，the reference wave can be expressed as

$$O_r(x,y) = \mathscr{F}^{-1}\{\mathscr{F}[O_o(x,y)] \times T_{PH}\}\exp[i\kappa(x,y)], \quad (1)$$

where $\mathscr{F}[\cdot]$ and $\mathscr{F}^{-1}[\cdot]$ denote the 2D Fourier transform and the 2D inverse Fourier transform，respectively. The term $\mathscr{F}\{\mathscr{F}[O_o(x,y)] \times T_{PH}\}$ denotes the average or non-diffracted component of the object wave obtained by the pinhole filtering. T_{PH} denotes the transmittance of the pinhole filter；$\kappa(x,y)$ is the spatial frequency induced by the tip/tilt of the mirror M1 respect to the optical axis. Here，the carrier frequencies can be determined from the fringes of the off-axis interferogram.

It should be noticed that the intensity of the reference wave is much lower than the intensity of the signal wave after the pinhole filtering. To ensure the best possible signal-to-noise ratio，the fringe contrast provided by the interferometer should be maximized. Either a variable neutral density filter or the coating method[14] can be applied，with which adjustable contrast of the fringe pattern can be realized by adjusting the relative intensities of interfering waves. For the slightly off-axis IPDI，the interference pattern recorded on the image plane can be written as

$$I(x,y) = I_b(x,y) + \gamma(x,y)\cos[k_x x + k_y y + \varphi(x,y)], \quad (2)$$

where $I_b(x,y) = |O_o(x,y)|^2 + |O_r(x,y)|^2$ and $\gamma(x,y) = 2|O_o(x,y)||O_r(x,y)|$ denote the background intensity and the modulation factor，respectively；$\varphi(x,y)$ is the phase delay due to the specimen.

In fact，the direct current (DC) component of the fringe can also be determined by subtracting the average intensity. After that，the proposed method effectively extracts the phase from a slightly off-axis fringe pattern by employing the windowed Fourier transform algorithm[15,16]:

$$O(x,y) = \frac{1}{4\pi^2}\int_{\eta_1}^{\eta_2}\int_{\xi_2}^{\xi_1} \{[I'(x,y) * h(x,y,\xi,\eta)] * h(x,y,\xi,\eta)\}\mathrm{d}\xi\mathrm{d}\eta, \quad (3)$$

where $O(x,y)$ denotes the complex amplitude distribution of the object wave；$h(x,y,\xi,\eta) = g(x,y)\exp(i\xi x + i\eta y)$ is the basis of windowed Fourier transfom，and $*$ denote the convolution with respect to the coordinates x and y. In this paper，the Gaussian window $g(x,y) = \exp[-(x^2 + y^2)/2\sigma^2]$ is chosen as the window function used for local frequency spectrum filtering；σ is the standard deviation of the Gaussian function. ξ and η are the spatial coordinates in the frequency domain. Phase ambiguities will still exist after the Fourier-transformed local frequency spectrum filtering. This is exactly the same phase unwrapping issue that exists in the standard

fringe analysis. Next, an unwrapping algorithm is applied to obtain the final wrapped object phase[17]. After removal of the 2π ambiguity by a phase unwrapping process, the total phase information can be obtained. By using the above mentioned reconstruction method, the phase distribution of the tested specimen is obtained.

Since WFPI is performed localized transform from pixel to pixel, it is more tolerant to the area of the wrapped phase map, and possesses both the advantages of the Fourier transform method and the localized Window filtering algorithm to eliminate the nonlinear errors of the fringe. As a result, the only limitation is the recording time of the detector.

4 Experiment and discussion

To demonstrate feasibility of the proposed system, the experiment of slightly off-axis interferometer for transmitted wavefront test is performed based on the experimental setup depicted in Fig. 1. The infrared camera (FLIR SC 2000, FLIR Systems) has a maximum acquisition rate of 206 frame/s at the full resolution of 320 pixel × 256 pixel and the pixel size of 30 μm × 30 μm. The L4-L5 lens system has the magnification of $f4/f5 = 3.3$, so that the cosine modulation of the fringe is approximately sampled by 10 pixel per period.

In our experiment, an entrance window designed for the adaptive wavefront sensor cryostat of VLTI was used as specimen. The whole process of the phase retrieval is demonstrated in Fig. 2. Fig. 2(a) shows the fringe formed in the IPDI setup as a result of the interference of the low-pass filter reference and the object beams. Fig. 2(b) shows that the complex amplitude of the object wave is retrieved by using windowed Fourier filtering method, where the phase is still wrapped. The reconstructed quantitative phase profile of the entrance optical window is obtained by subtraction of the background and is depicted in Fig. 2(c).
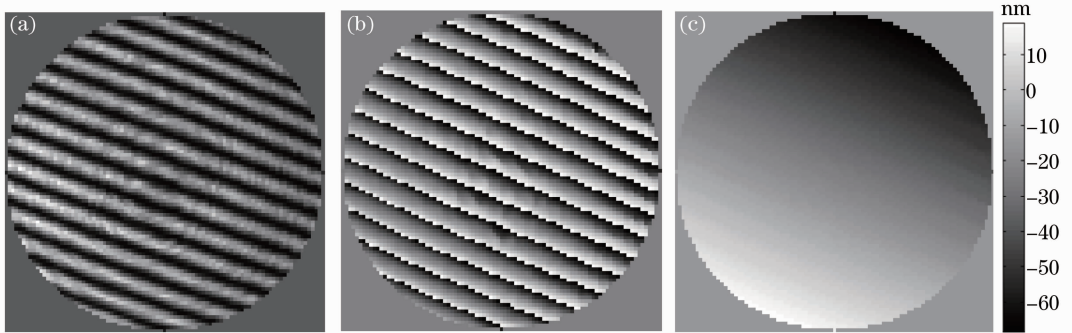

Fig. 2 Experimental results based on off-axis infrared point-diffraction interferometer. (a) Typical slightly off-axis interferogram of a multi-layer coated optical window; (b) wrapped phase distribution extracted by the windowed Fourier transformed spatially filtered method; (c) reconstructed object wave.

The measurement was taken without the presence of the specimen in order to calibrate the instrument. This background phase subtraction allows us to correct the residual errors associated with experimental setup. Using these data, the wrapped background phase can be calculated. Fig. 3(a) presents a quantitative transmitted optical-path difference (OPD) of the entrance window after the OPD of setup is subtracted. The reconstructed wavefront deformation [see Fig. 3(b)] is represented by a set of orthogonal functions with suitable coefficients[17]. Here the Zernike polynomials are implemented as the sets of orthogonal function.

To quantify the stability of the instrument against environmental disturbances, and thus identify the repeatability of measurements, we continuously measured sets of 100 frames without the sample, with intervals of 18 s (covering in total 30 min). The integration time of infrared camera is about 10 ms for each frame. The standard deviation of the optical-path difference associated with the full field of phase map is a standard deviation of 0.20 nm, as shown in Fig. 4(a). An arbitrary 4 pixel × 4 pixel average point, characterized by a standard deviation of 0.13 nm, is also shown in Fig. 4(b). The repeatability obtained during preliminary tests is better than several nanometers in root-mean-square (RMS) for the wavefront phase measurement.
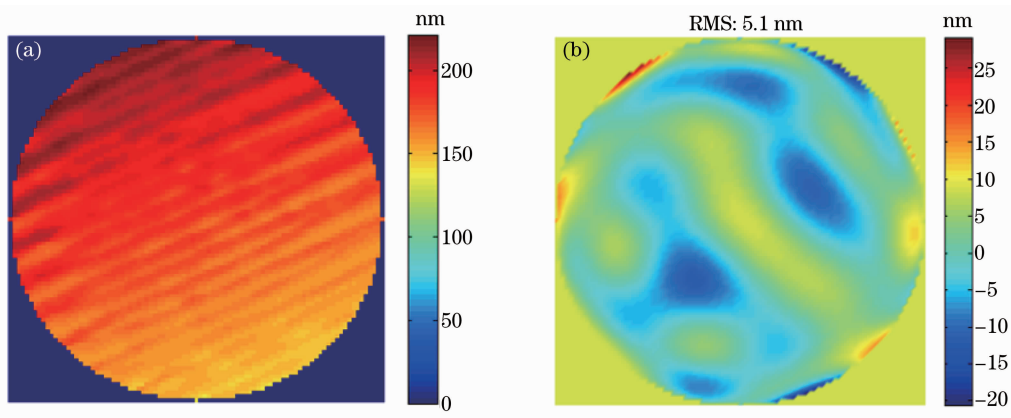
Fig. 3　Measured transmitted wavefront error of the opical window. （a）Optical path difference of the blocking filter after calibration；（b）Zernike fitting of the wavefront deviation of a central circular part of the blocking filter with a diameter of 15 mm. The Zernike fitting is calculated to a maximum of 10，and the focus and offsets（tip，tilt）have been removed.
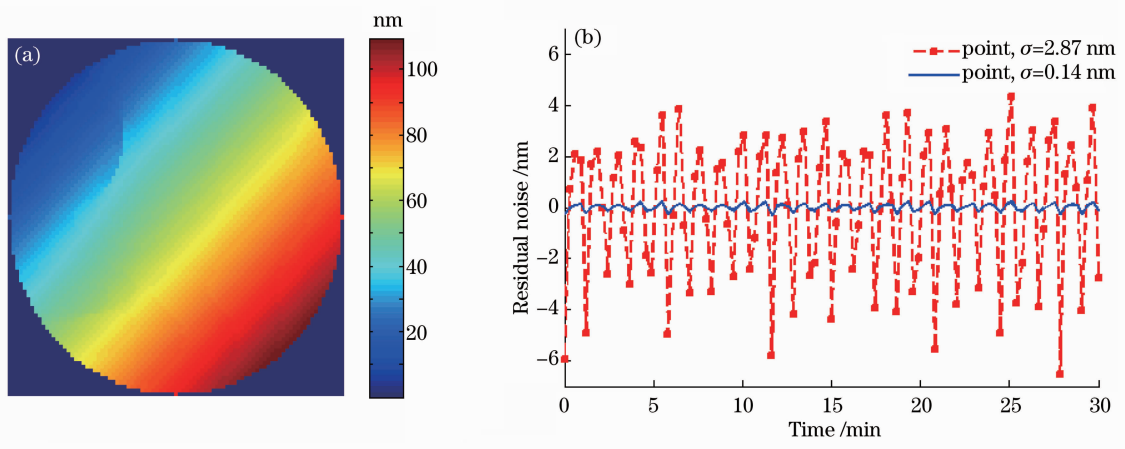

Fig. 4　Stability test for the proposed setup in nanometers associated with the background of the full field of view（red dashed line）and a single point phase profile（blue solid line）.
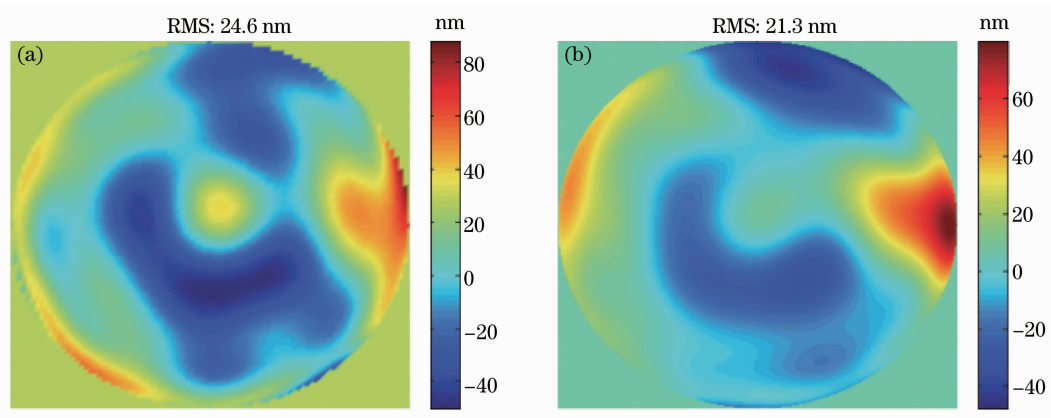

Fig. 5　Quantitative phase maps of the normal BK7 optical window measured by（a）infrared point-diffraction interferometer and（b）phase shifting Twyman-Green interferometer.

We also compared quality of the phase measurement results of the prototype step phase-shifting interferometer with our proposed setup. A BK7-made optical window transmitting both in optical and infrared region was used as a specimen. The RMS values of the results obtained by the proposed method

[Fig. 5（a）] and that by using μphase interferometer （TRIOPTICS GmbH，Germany）[Fig. 5（b）] were 24.6 nm and 21.3 nm，respectively，which shows great consistency with each other.

5　Conclusion

In this paper，we presented infrared point-diffraction interferometer as a novel approach to study the transmitted wavefront quality of the silicon optical windows，which combines the high spatial resolution associated with slightly off-axis feature and intrinsic windowed Fourier spatial analysis techniques. The proposed IPDI is compact，vibration-insensitive，and sufficient for the dynamic process measurement. The major advantage of the setup is the simplicity，high temporal stability and its potential low cost. In the slightly off-axis IPDI experiment，the certain spatial resolution of the test specimen is well preserved，and the instrument presented here requires only simple components in comparison with other proposed setups[4~12]. These advantages could be attractive for many other applications and will enable new advances in wavefront sensing for astronomical science.

References

1 R. N. Smartt，W. H. Steel. Theory and application of point diffraction interferometers [J]. *Jpn. J. Appl. Phys.*，1975，**14**(1)：351~356

2 Osuk Y. Kwon. Multichannel phase-shifted interferometer [J]. *Opt. Lett.*，1984，**9**(2)：59~61

3 Guiying Wang，Yanling Zheng，Aimin Sun *et al.*. Polarization pinhole interferometer [J]. *Opt. Lett.*，1991，**16**（17）：1352~1354

4 Mark J. Guardalben，Lutao Ning，Nieraj Jain *et al.*. Experimental comparison of a liquid-crystal point-diffraction interferometer （LCPDI）and a commercial phase-shifting interferometer and methods to improve LCPDI accuracy [J]. *Appl. Opt.*，2002，**41**(7)：1353~1365

5 Sang Hun Lee，Patrick Naulleau，Kenneth A. Goldberg *et al.*. Phase-shifting point-diffraction interferometry at 193 nm [J]. *Appl. Opt.*，2000，**39**(31)：5768~5772

6 Robert M. Neal，James C. Wyant. Polarization phase-shifting point-diffraction interferometer [J]. *Appl. Opt.*，2006，**45**(15)：3463~3476

7 Peng Gao，Irina Harder，Vanusch Nercissian *et al.*. Phase-shifting point-diffraction interferometry with common-path and in-line configuration for microscopy [J]. *Opt. Lett.*，2010，**35**（5）：712~714

8 Gabriel Popescu，Takahiro Ikeda，Ramachandra R. Dasari *et al.*. Diffraction phase microscopy for quantifying cell structure and dynamics [J]. *Opt. Lett.*，2006，**31**(6)：775~777

9 C. Joenathan，G. Pedrini，I. Alekseenko *et al.*. Novel and simple lateral shear interferometer with holographic lens and spatial Fourier transform [J]. *Opt. Eng.*，2012，**51**(7)：075601

10 Matt Novak，James Millerd，Neal Brock *et al.*. Analysis of a micropolarizer array-based simultaneous phase-shifting interferometer [J]. *Appl. Opt.*，2005，**44**(32)：6861~6868

11 Chenguang Zhao，Jiubin Tan，Jianbo Tang *et al.*. Confocal simultaneous phase-shifting interferometry [J]. *Appl. Opt.*，2011，**50**(5)：655~661

12 Rongli Guo，Baoli Yao，Peng Gao *et al.*. Reflective point-diffraction microscopic interferometer with long-term stability [J]. *Chin. Opt. Lett.*，2011，**9**(12)：120002

13 S. Kendrew，S. Hippler，W. Brandner *et al.*. GRAVITY coudé infrared adaptive optics （CIAO）system for the VLT interferometer [C]. *SPIE*，2012，**8446**：84467W

14 K. Otaki，T. Yamamoto，Y. Fukuda *et al.*. Accuracy evaluation of the point diffraction interferometer for extreme ultraviolet lithography aspheric mirror [J]. *J. Vac. Sci. Technol. B*，2002，**20**(1)：295~300

15 P. Yang，S. Hippler，C. P. Deen *et al.*. Optimizing the transmission of the GRAVITY/VLTI near-infrared wavefront sensor [C]. *SPIE*，2012，**8445**：844531

16 K. Qian. Windowed Fourier transform method for demodulation of carrier fringes [J]. *Opt. Eng.*，2004，**43**(7)：1472~1473

17 Jan Herrmann. Least-squares wave front errors of minimum norm [J]. *J. Opt. Soc. Am.*，1980，**70**(1)：28~35